Applied Catalysis B: Environmental 89 (2009) 22–32

Contents lists available at ScienceDirect

Applied Catalysis B: Environmental

journal homepage: www.elsevier.com/locate/apcatb

Catalytic combustion of butane on Ru/γ-Al_2O_3 catalysts

Janina Okal *, Mirosław Zawadzki

Institute of Low Temperature and Structure Research, Polish Academy of Sciences, P.O. Box 1410, 50-950 Wrocław, Poland

ARTICLE INFO

Article history:
Received 26 September 2008
Received in revised form 13 November 2008
Accepted 14 November 2008
Available online 25 November 2008

Keywords:
Catalytic combustion
Butane
Ru/γ-Al_2O_3 catalysts
Chlorine
Pre-treatment effect

ABSTRACT

Ru/γ-Al_2O_3 catalysts were prepared by incipient wetness method from $RuCl_3$ precursor and their performance in oxidation of *iso*- and *n*-butane was investigated. The catalytic activity was examined on the calcined–reduced and on the directly reduced catalysts, with and after removing Cl ions, as well as after the oxidation at 250 °C. All catalysts have been characterized by various methods such as BET, XRD, TEM, XPS, H_2 chemisorption and O_2 uptake in order to correlate their performance with their physiochemical properties. It was found that pre-treatment procedure has a significant influence on activity of the Ru/γ-Al_2O_3 catalysts. The considerable contamination of Ru particles by chlorine ions results in lowering activity of the Ru/γ-Al_2O_3 catalysts. It was established that reduced nearly Cl-free Ru/γ-Al_2O_3 catalysts exhibited higher activity than catalysts oxidized at 250 °C. It was shown by XRD, TEM and O_2 uptake data that at this temperature, very small Ru particles were transformed completely into RuO_2, while the large Ru particles were partly covered by a thin RuO_2 film (1.6 nm). Catalytic and characterization results revealed that the most active sites in the butane oxidation reaction, consist probably of a few layers of thick surface oxide on the large Ru particles and small Ru_xO_y clusters without well-defined stoichiometry. Such surface species were formed at 100–200 °C in all catalysts and in the most active reduced Cl-free 4.6% Ru catalyst which reached 100% butane conversion below 200 °C. The catalytic performance of Ru declined as the catalysts were oxidized at higher temperature. The activity loss was attributed to the formation of crystalline RuO_2 phase and to some sintering of the active phase. In the used catalysts, small Ru particles were oxidized to RuO_2 while the large Ru particles were covered with RuO_2 layer, with a thickness of 2–3 nm, as shown by TEM and XRD.

1. Introduction

Volatile organic compounds (VOCs) include a large range of chemicals such as hydrocarbons with several functional groups, which could be originated from various sources but mainly from vehicles and various industrial processes (chemical, petrochemical, manufacturing of paints, plastics, etc.). VOCs being one of the main pollutants of the air are an important environmental problem because some of them are directly harmful (carcinogenic, mutagenetic, etc.) and cause other social destructions such as ozone layer depletion, green house effect and so on [1–3].

Many technologies, that have been developed to provide the destruction of those toxic compounds at low concentrations in industrial gaseous effluent, use deep oxidation as a more advantageous, safe treatment method, because the oxidation products are mainly carbon dioxide and water, and conversion is quite fast [4]. Thermal oxidation was first implemented for the VOCs elimination, but it proceeds at high temperatures (higher than 800 °C) and can result in the formation of some compounds (dioxins, carbon monoxide, nitrogen oxides, etc.) even more dangerous than the ones to be eliminated. The catalytic oxidation is a more attractive way to eliminate VOCs since it offers the possibility of their removal from aerial effluents to very low levels (high cleaning efficiency) and much lower temperature is required what results in more economical process with significantly reduced potential for the production of toxic by-products.

Currently, the most active catalysts at low temperature VOCs combustion are based on noble and transition metals. Platinum, palladium and rhodium are generally dispersed on supports with high specific surface area such as alumina and titania [5,6], silica [7] or activated carbon [8]. These systems exhibit high activities and selectivities at low temperature, but they are unstable in the presence of chloride compounds [9]. Other systems are based on transition metal oxides and are generally less active but more resistant towards poisoning and their cost is also significantly lower. They are usually supported on porous oxides [10,11] or used as bulk catalysts without support [12]. Mixed oxide such as MnO_x-CeO_2 and others have been also extensively studied as catalysts for eliminating VOC emission [13]. There still remains a scope for further investigation and development of improved catalysts for effective VOCs combustion.

* Corresponding author. Tel.: +48 71 34 350 20; fax: +48 71 34 410 29.
E-mail addresses: J.Okal@int.pan.wroc.pl (J. Okal), M.Zawadzki@int.wroc.pl (M. Zawadzki).

0926-3373/$ – see front matter © 2008 Elsevier B.V. All rights reserved.
doi:10.1016/j.apcatb.2008.11.024

Supported ruthenium catalysts have received much attention over the past years, because of their high activity in oxidation as well as reduction reactions. Ruthenium catalysts, especially these containing Ru dioxide, offer good thermal and chemical stability, strong resistance to chemical corrosion and excellent chemical diffusion barrier [14,15]. Supported Ru catalysts have been proved to be among the best catalytic systems for oxidation of various substrates, to name but a few: methane [16,17], carbon monoxide [18–20], ammonia [21], hydrogen [22], alcohols [23], diesel soot [24], and even in low temperature oxidation of HCl [15]. Furthermore Ru catalysts are also known to be active in various other catalytic reactions such as ammonia synthesis, water–gas shift reaction, steam reforming and reduction of NO by hydrocarbons [25–27]. However, few studies on VOCs combustion over supported Ru catalysts have been conducted so far. Only wet air oxidation of VOCs has been well documented in the literature [28–31], but this method seems to be inappropriate for practical use since highly pressurized conditions are needed to oxidize VOCs at low temperature. Combustion over Ru catalysts in gas phase under atmospheric pressure was investigated for some volatile organic compounds such as toluene, ethyl acetate, acetaldehyde, and *ortho*-xylene [32] but only few studies investigated their reactivity in light alkane combustion [33,34].

Although VOCs are a wide ranging class of chemicals (over 300 compounds are now classed as VOCs by US EPA), it is clear from numerous studies that linear short chain alkanes are the most difficult to destroy [6,35]. It is also known that these VOCs, emitted mainly by natural gas fueled vehicles and gas power plants, have much larger detrimental greenhouse effect than carbon dioxide. Therefore, in the present work the catalytic performance of Ru supported on γ-alumina was evaluated in the total oxidation of butane, selected as a VOC probe molecule. Catalysts containing various amounts of ruthenium were prepared, and the influence of the pre-treatment procedure on the their physiochemical characteristics and catalytic activity in combustion of *iso*- and *n*-butane mixture at low concentration has been studied.

2. Experimental

2.1. Catalyst preparation

The Ru/γ-Al_2O_3 catalysts were prepared by the incipient wetness impregnation method using an aqueous solution of $RuCl_3 \cdot 3H_2O$ (Koch and Light) and γ-Al_2O_3 with BET surface area of 245.9 m^2/g and pore volume of 0.21 cm^3/g. Following impregnation and drying at 110 °C, the samples were subjected to two different types of pre-treatments protocols, i.e., direct reduction in hydrogen or calcination–reduction treatment. Preparation details of the directly reduced catalysts, with the metal loading of 4.6 and 10.8 wt.%, had previously been described [36,37]. Shortly, the samples after drying were reduced in hydrogen flow at 500 °C for 20 h. Next, each catalyst sample was divided into two parts. The first part of the catalyst was used without any treatment to elucidate the effect of residual chlorine on the oxidation activity of the catalyst (unwashed catalysts). The second part of the directly reduced catalyst was washed several times with hot distilled water to remove chlorine ions, next dried at 110 °C and again reduced in H_2 flow at 500 °C for 5 h (washed catalyst). In the second activation protocol, after impregnation and drying, the sample with ruthenium loading of 3.5 wt.%, was first calcined in air at 400 °C for 3 h, then washed several times with hot distilled water, and finally reduced in hydrogen flow at 500 °C for 20 h (calcined–reduced catalyst). In contrast to the directly reduced samples, in this preparation route, Cl^- ions were detected neither by XPS nor by chemical analysis.

Additionally, the Ru/γ-Al_2O_3 catalysts after reduction treatment, were heated in air at 250 °C (5 °C/min) for 1 h prior to activity measurements or characterization studies. The selected reduced samples were also heated in air at higher temperature.

2.2. Chemical analyses

The Ru loading in the catalysts, both after treatment in hydrogen, and in air at different temperature, was determined by the ICP-AES method. For the Ru/γ-Al_2O_3 catalysts treated in an oxidizing atmosphere to 400 °C or even to 600 °C, no loss of the Ru metal was noticed. Thus, the volatile Ru oxides were not formed under applied conditions. Chlorine content in the catalyst before and after washing procedure, as well as, in the solution after washing was determined by ion selective electrode.

2.3. Characterization techniques

The BET surface area of the samples was measured by N_2 adsorption at −196 °C using classical volumetric glass apparatus. Before the measurements, the catalyst samples were degassed at 300 °C for 3 h.

X-ray diffraction patterns (XRD) were obtained using a DRON-3 diffractometer with a Ni-filtered Cu Kα radiation. Diffraction patterns were recorded over 2Θ range from 10° to 80° and a speed of 0.5° min^{-1}. The ICDD database [38] was used for phase identification.

Transmission electron microscopy (TEM) was employed to study the microstructure of both the reduced and oxidized at 250 °C Ru/γ-Al_2O_3 catalysts, and the samples after activity measurements. TEM and HRTEM images and selected area electron diffraction (SAED) patterns were recorded with Philips CM20 SuperTwin microscope, which at 200 kV provides 0.25 nm resolution. The specimens for TEM were prepared by grinding of the powdered catalyst in a mortar, dispersing it in methanol and placing a droplet of the suspension onto a copper grid covered with perforated carbon.

The composition of the Ru catalyst surfaces was analyzed by X-ray photoelectron spectroscopy (XPS), performed on the UHV SPECS system equipped with a PHOIBOS-100 spectrometer, SpecLab software and with a Mg anode [36]. The binding energy scale was calibrated to the Al 2p peak at 74.4 eV.

The dispersion of ruthenium was determined by the H_2 chemisorption method at 100 °C using the conventional volumetric glass apparatus employed earlier (base pressure 10^{-6} Torr) [36]. Before chemisorption measurements, the sample of the catalyst (∼1 g) was first reduced with H_2 at 400 °C for 2 h then degassed at 400 °C and 10^{-6} Torr for 2 h. After cooling under vacuum to the adsorption temperature, hydrogen adsorption isotherms (total and reversible) were measured as described in ref. [36].

The extent of the Ru oxidation in selected catalyst samples at room temperature (RT) and at 250 °C was determined by the oxygen uptake measurements [39] using the same apparatus as in the H_2 chemisorption. The sample was first reduced at 400 °C for 2 h, degassed at the same temperature for 2 h and cooled under vacuum to RT. Then, oxygen was introduced and the amount of O_2 adsorbed at room temperature was determined at 80–160 Torr. Next, the temperature was raised to 250 °C, and the sample was kept in the isothermal conditions for 1 h. After cooling the sample under oxygen to RT, the total O_2 uptake was measured.

2.4. Catalytic experiments

The catalytic reaction was carried out in a fixed-bed flow reactor, made of quartz tubing of 10 mm inner diameter, placed in

a programmable furnace, by passing a gaseous mixture of C_4 alkane (*n*-butane: 55 vol.%, *iso*-butane: 45 vol.%) and air over 700 mg catalyst. Measurements were taken as the samples were heated stepwise at the temperature in the range of 25–450 °C. Before the test, each catalyst was first pressed and compacted, and then crushed and sieved to the desired size. A gaseous mixture of butane and air was fed at a flow rate of 15 l/h and catalysts were packed to a constant volume to give a gas hourly space velocity GHSV of 21,000 h^{-1} for all studies. The gas flow was adjusted by mass flow controllers and the volumetric ratio used for the catalytic combustion was C_4/air = 1:500. The combustion products were analyzed on-line using a gas chromatograph (Chromatron GCHF 18.3) with a flame ionization detector (FID) using nitrogen as the carrier gas. *Conversion* data were calculated by the difference between inlet and outlet concentrations. Activity measurements were obtained once steady state was attained and the data are an average of at least 3 consistent analyses. The conversion data were reproducible within 5% accuracy. Products of the reaction were CO_2 and H_2O. No CO or other peaks attributed to other compounds were observed. Blank runs showed no conversion in the studied temperature interval.

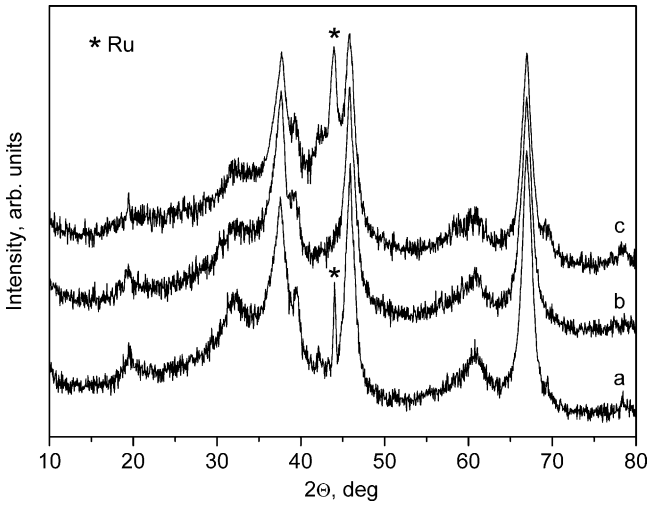

Fig. 1. X-ray diffraction patterns of the catalysts (a) 3.5% Ru/γ-Al_2O_3 (calcined–reduced), (b) 4.6% Ru/γ-Al_2O_3 (reduced) and (c) 10.8% Ru/γ-Al_2O_3 (reduced).

3. Results and discussion

3.1. General characteristics of the catalysts before activity studies

The BET surface areas and ruthenium dispersion data obtained from hydrogen chemisorption are shown in Table 1. The BET surface areas of the unwashed catalysts (4.6% and 10.8 wt.% Ru) were significantly lower than that of bare support or the same catalysts after the washing procedure. As expected, considerable amount of Cl was retained in the unwashed catalysts after reduction treatment at 500 °C, though the washing procedure with hot water strongly decreases, but did not eliminate completely, the chlorine content [36,37]. However, application of the calcination–reduction protocol in the preparation of the 3.5% Ru/γ-Al_2O_3 catalyst did not make Cl ions retain on the catalyst surface. The changes in the BET surface areas of the directly reduced samples had previously been explained [36,37] by some dissolution of the alumina support during the impregnation with the $RuCl_3$ aqueous solution and its further deposition at the surface of the alumina, causing partial pore mouth blockage. Hydrogen chemisorption data included in Table 1 show that Ru dispersion is improved in the washed 4.6% and 10.8% Ru/γ-Al_2O_3 catalysts. However, as we had reported earlier, the contamination of ruthenium surface by chlorine ions or by the support material causes that metal dispersion determined by H_2 chemisorption may be significantly underestimated [36]. The low Ru dispersion obtained for the 3.5% Ru/γ-Al_2O_3 catalyst (H/Ru = 0.07) contradicts the general rule that the dispersion of a lightly loaded metal catalyst is larger than that of a more heavily loaded one. Thus, the results of Table 1 indicate that the pre-treatment procedure of the Ru catalysts have a significant influence on the Ru dispersion.

3.2. X-ray diffraction studies

XRD patterns of the calcined–reduced 3.5% Ru/γ-Al_2O_3 catalyst and the directly reduced 4.6 and 10.8% Ru/γ-Al_2O_3 catalysts after washing procedure and the same samples after oxidation at 250 °C are presented in Figs. 1 and 2, respectively. The patterns of the reduced catalysts, with metal loading of 3.5 and 10.8 wt.% Ru, contain strong reflections of metallic phase (Fig. 1, traces a and c). The pattern of the 4.6% Ru/γ-Al_2O_3 catalyst (Fig. 1, trace b) contains only reflections from alumina indicating that Ru forms very small particles dispersed on the support. It was found that the washing procedure did not change the XRD patterns of the catalyst samples. The mean Ru crystallite size determined from the line broadening of the strongest Ru (1 0 1) reflection at $2\Theta = 44°$ (by the Scherrer formula) is 7.0 and 18 nm for the 10.8% and 3.5% Ru/γ-Al_2O_3 catalyst, respectively. In accordance to chemisorption data, the X-ray diffraction results show that the pre-treatment procedure of the catalysts have a significant influence on the Ru crystallite size (see Table 1). In particular, in the sample that was subjected to the calcination in air before reduction process, severe sintering of the metal phase occurs. Similar sintering effects caused by the calcination treatment of the Ru/Al_2O_3 catalysts had been previously reported in the literature [40–42]. For example, Han et al. [41] found that calcination/reduction treatment at 350 °C of the Ru/Al_2O_3 catalyst results in the particle sintering (d_{av} = 11.2 nm), while direct reduction in H_2 does not lead to particle growth (d_{av} = 2.5 nm).

The patterns of the catalysts oxidized at 250 °C for 1 h, with metal loading of 4.6 and 10.8 wt.% Ru (Fig. 2, traces b and c), shows the characteristic reflections corresponding to RuO_2 oxide (JCPDS 88-0322), with (1 1 0), (1 0 1) and (2 1 1) as the prevailing primary

Table 1
Characterization data for the Ru/γ-Al_2O_3 catalysts.

Catalyst	BET[b] (m^2/g)	Irreversible H_2 uptake (μmol/g cat.)	Dispersion[c] (H/Ru)	d_{av} (TEM) (nm)	d_{av} (XRD) (nm)	Cl content (wt.%)
3.5% Ru/γ-Al_2O_3 (calcined/reduced)	215.0	12	0.07	4.7	18	Trace
4.6% Ru/γ-Al_2O_3[a] (unwashed/reduced)	183.5	36	0.16	2.6	Not visible	4.0
4.6% Ru/γ-Al_2O_3[a] (washed/reduced)	219.3	53	0.23	2.5	Not visible	0.4
10.8% Ru/γ-Al_2O_3 (unwashed/reduced)	164.6	47	0.09	3.4	6.9	4.9
10.8% Ru/γ-Al_2O_3 (washed/reduced)	210.2	61	0.11	3.2	7.0	0.8

[a] Data from ref. [36].
[b] The BET surface area of the pure γ-Al_2O_3 amount to 245.9 m^2/g and pore volume of 0.21 cm^2/g.
[c] Dispersion of ruthenium is defined as the ratio of exposed Ru surface atoms to the total number of Ru atoms, assuming $H/Ru_s = 1$ [36].

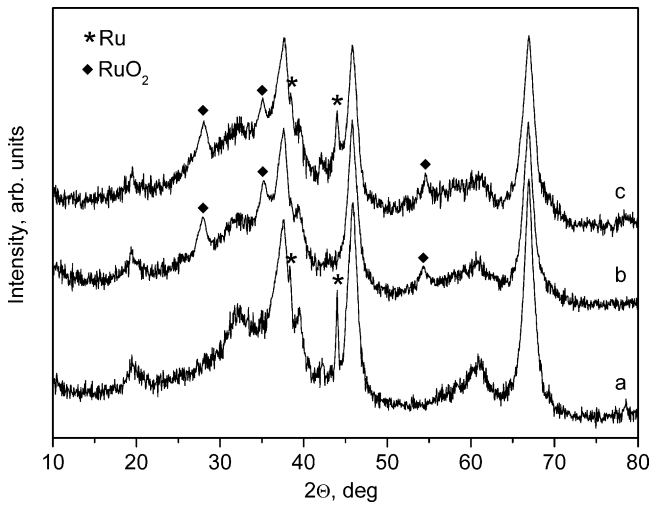

Fig. 2. X-ray diffraction patterns of the catalysts after oxidation treatment at 250 °C (a) 3.5% Ru/γ-Al_2O_3, (b) 4.6% Ru/γ-Al_2O_3 and (c) 10.8% Ru/γ-Al_2O_3.

orientations. Additionally, the 10.8% Ru catalyst contains also reflections of the metallic Ru. In both catalysts, the mean crystallite size of the ruthenium oxide, calculated from the line broadening of the most intense (1 1 0) reflection of the RuO_2 phase at $2\Theta = 28.0^\circ$ is similar, and amounts to about 4–5 nm. No evidence of any Ru oxide phase was found for the 3.5% Ru/Al_2O_3 catalyst (Fig. 2, trace a), and the pattern contains only the reflections of the metallic ruthenium. Nevertheless, ruthenium oxide in this sample may exist as an amorphous or highly dispersed phase or as a thin film on the top of the metallic ruthenium particles, not giving detectable diffraction peaks. Thus, XRD data suggest that the small Ru particles are more susceptible to full oxidation than the large Ru particles. For this reason, the intensity and width of the Ru^0 reflections changed for the catalyst with the 10.8% metal loading, as compared to the reduced sample (cf. Figs. 1c and 2c). The XRD data evidently show an increase of the average crystallite size of metallic Ru during the oxidation treatments at 250 °C, i.e., from 7.0 to 11.3 nm after oxidation, possibly due to complete oxidation of the smallest Ru nanoparticles. Vogel and Alonso-Vante [43] found that above 70 °C small Ru clusters (2.8 nm) could be oxidized to an amorphous Ru_xO_y phase. In accord with our XRD data, Bond et al. [44] found, for highly dispersed Ru/Al_2O_3 catalysts, that the RuO_2 phase began to appear at 230 °C. Very similar XRD patterns were obtained for the unwashed catalyst samples (not shown).

3.3. TEM studies

Representative TEM images and SAED patterns (insets) of the calcined–reduced 3.5% Ru/γ-Al_2O_3 catalyst and directly reduced 4.6 and 10.8% Ru/Al_2O_3 catalysts after washing procedures are shown in Fig. 3. In size distributions of Ru particles calculated from TEM micrographs are given also as insets to Fig. 3. In all SAED patterns only continuous rings corresponding to γ-Al_2O_3 and individual spots assigned to metallic Ru are present. TEM images show that in all samples Ru particles were not uniformly distributed over the support and for 3.5% and 10.8% Ru catalysts (Fig. 3a and c) exhibited a broad size distribution (in range of 1–24 nm). Occasionally, in the sample with the Ru loading of 3.5%, particles with sizes up to 35 nm were also detected. The mean size of Ru particles was calculated on the basis of size measurements of 300–400 particles for each sample. The measurements were done manually using the ImageJ program [45]. The mean particle size of 4.7 nm was obtained for the 3.5% Ru catalyst and 2.5 and 3.2 nm for the directly reduced 4.6% and 10.8% Ru/γ-Al_2O_3 catalysts, respectively. However, except for the catalyst with the Ru content of 4.6 wt.%, the mean particle size estimated from TEM deviates significantly from that obtained by XRD technique (see Table 1). This discrepancy should be attributed to the difference in the Ru particle size distribution in the catalysts, because the experimental results give only an average value over the distribution. As shown in Fig. 3, the number of the Ru particles smaller than ca. 3 nm, which are not observable by XRD measurement, was significantly greater on the 10.8% Ru/γ-Al_2O_3 catalyst than that of on the 3.5% Ru/γ-Al_2O_3 catalyst. TEM images of the unwashed samples were similar to those presented in Fig. 3b and c, and are not shown.

TEM observation of the samples oxidized at 250 °C (not shown) revealed that the overall morphology of the given catalyst was similar to that of the reduced sample (see Fig. 3). Also, the SAED patterns from the 3.5% and 10.8% Ru/γ-Al_2O_3 catalysts oxidized at 250 °C, were very similar to those presented in Fig. 3a and c, i.e., only alumina rings and spots from metallic Ru were present. However, recent HRTEM studies of the 10.8% Ru/γ-Al_2O_3 catalyst [39] showed that the large metal particles were covered with 1.6-nm thick oxide layer. Only in the SAED pattern (not shown) of the 4.6% Ru/γ-Al_2O_3 catalyst oxidized at 250 °C, weak diffraction spots from both the Ru metal and RuO_2 oxide phases were present. Also, the presence of small well-crystallized particles is clearly seen in a HRTEM image of the 4.6% Ru/Al_2O_3 catalyst oxidized at this temperature (Fig. 4). The fast Fourier transform (FFT) pattern (insets in Fig. 4) from the particle signed as "*a*" contains spots corresponding to RuO_2 (1 1 0) (0.32 nm lattice fringes), whereas FFT pattern from the particle signed as "*b*" contains spots corresponding to Ru (0 1 0) and Ru (1 0 0) (for both 0.23 nm lattice fringes). Thus, in accord with the XRD data, the small Ru particles in the Ru/Al_2O_3 catalysts could be completely oxidized to RuO_2, whereas the large ruthenium particles were covered with a poorly ordered layer of a ruthenium oxide, with a thickness of about 1.6 nm.

3.4. Uptake of oxygen

The results of the oxygen uptake (in μmol per 1 g of the catalyst) by the washed 4.6% and 10.8% Ru/γ-Al_2O_3 catalysts, as well as by the calcined–reduced 3.5% Ru/γ-Al_2O_3 catalyst, at RT and at 250 °C are presented in Table 2. Based on these volumetric data, the degree of ruthenium oxidation in these samples was calculated. The O_2 uptake for all catalysts at RT was low and it may be attributed to dissociative chemisorption on ruthenium surface [46–48]. However, the O_2 uptake on a given catalyst is approximately two times higher than H_2 uptake for the same sample (see Table 1), indicating that the surface oxide close to RuO_2 is formed on the ruthenium particles. Assmann et al. [49] found also by the O_2 chemisorption measurements, performed on highly dispersed Ru/MgO and Ru/SiO_2 catalysts, that a thin RuO_2 surface layer was formed on the ruthenium particles at room temperature. The O_2 uptake significantly increased on raising temperature to 250 °C, but in all samples ruthenium metal was not fully oxidized to the stable RuO_2 phase. As shown in the last column of Table 2, the amount of oxygen consumed at this temperature is much lower than the theoretical value, calculated by assuming the total oxidation of Ru to RuO_2. At 250 °C, only 50%, 34% or 30% of the total amount of ruthenium was oxidized to RuO_2 in the 4.6%, 10.8% and 3.5% Ru/γ-Al_2O_3 catalysts, respectively. Correspondingly, the total consumption of oxygen at 250 °C yielded O/Ru ratios of 1.0, 0.67 and 0.46, respectively. Thus, the O_2 uptake results may indicate the formation of a superficial Ru oxide at this temperature. However, when the XRD, TEM and O_2 uptake data are taken into account, it can be concluded that the

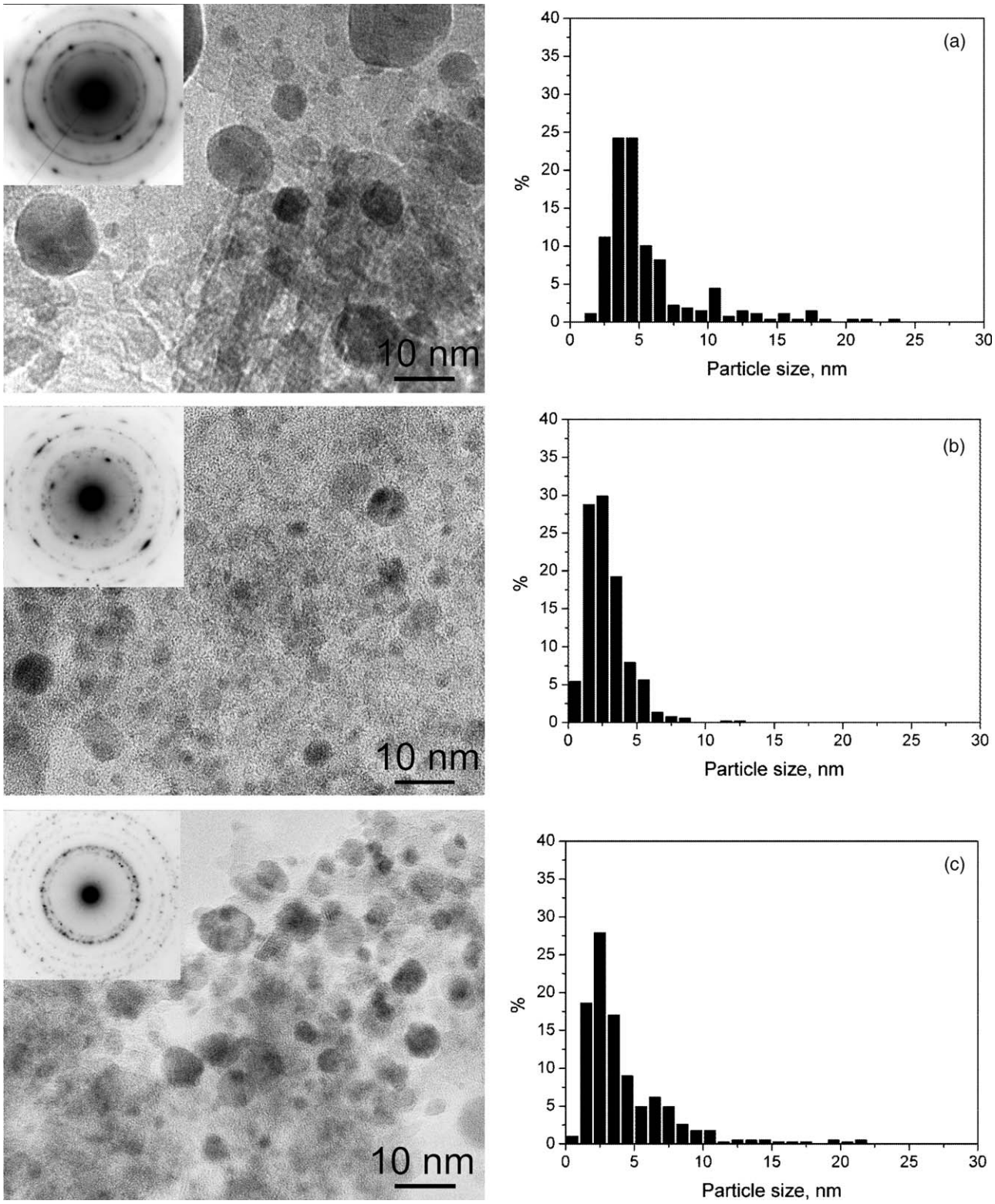

Fig. 3. TEM micrographs with SAED patterns (inset) and corresponding particle size distribution of the reduced catalysts (a) 3.5% Ru/γ-Al_2O_3, (b) 4.6% Ru/γ-Al_2O_3 and (c) 10.8% Ru/γ-Al_2O_3.

very small Ru particles are transformed completely into RuO_2 oxide, while the large Ru particles are only partly covered by a thin RuO_2 film, and there still remains a small core of the reduced metal. Very recently, a core–shell model for the Ru/SiO_2 catalyst under oxidizing reaction conditions was also proposed by Assmann et al. [19].

3.5. X-ray photoelectron spectroscopy studies

The XPS technique was employed additionally to establish the oxidation states of the surface ruthenium atoms in the selected Ru/γ-Al_2O_3 catalysts before activity measurements. As an example, Fig. 5 presents the XPS spectra (Ru 3p line) of the

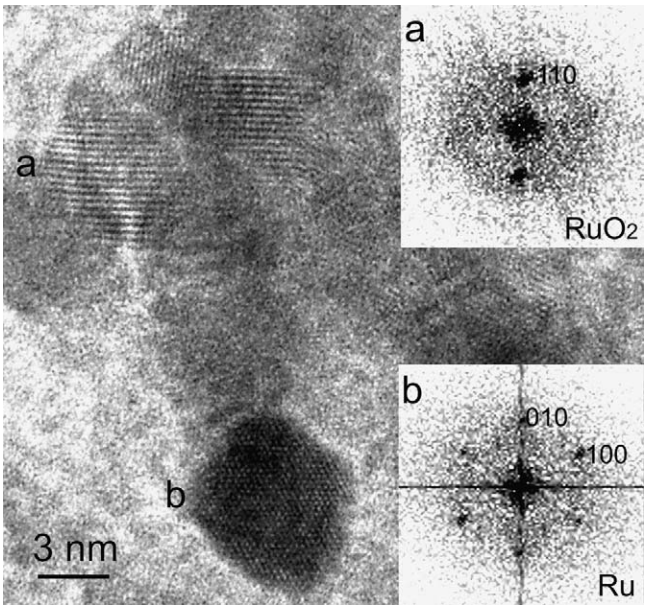

Fig. 4. HRTEM image of the washed 4.6% Ru/Al_2O_3 catalyst after oxidation at 250 °C and FFT patterns obtained from crystallites *a* and *b* are shown as insets.

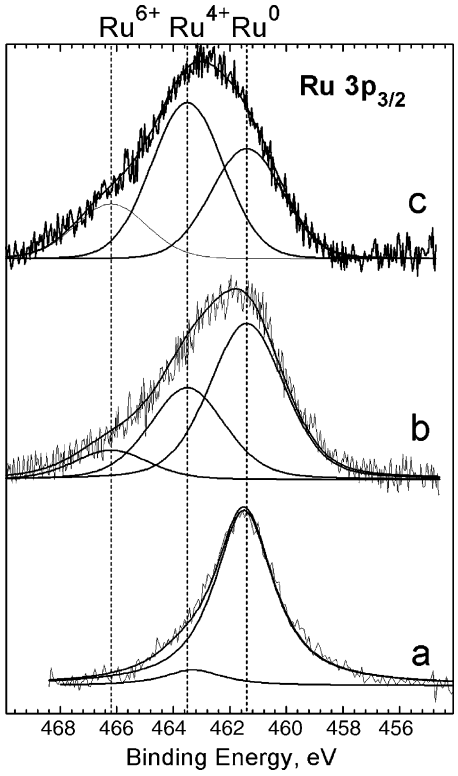

Fig. 5. XPS $3p_{3/2}$ spectra of (a) Ru metallic powder (as reference), (b) the washed 10.8% $Ru/\gamma\text{-}Al_2O_3$ catalyst after oxygen adsorption measurement at RT and (c) after oxidation at 250 °C for 1 h.

washed 10.8% $Ru/\gamma\text{-}Al_2O_3$ catalyst after the O_2 uptake measurements at RT and at 250 °C. The spectrum of the ruthenium powder (Ru 3p binding energy of 461.5 and 463.7 eV) is also included as a reference for Ru^0. Spectra of the catalyst show strong broadening of the Ru 3p peak. The shape and position of the peak show clearly that Ru^0 is a major phase of the catalyst after O_2 adsorption at RT and that the metallic phase is still present in the sample oxidized at 250 °C. After a careful deconvolution three ruthenium species could be detected. The peak at 461.5 is assigned to the Ru $3p_{3/2}$ line of Ru^0, but the two signals at higher binding energy could be assigned to Ru^{4+} and Ru^{6+}.

Table 3 shows the Ru^0/Ru^{n+}, Ru/Al and Cl/Ru surface atomic ratios obtained from XPS data of the selected catalysts. As expected, the extent of the surface oxidation of ruthenium significantly increases with the oxidation temperature. Moreover, a fraction of the oxidic Ru species was higher in the washed 4.6% $Ru/\gamma\text{-}Al_2O_3$ catalyst oxidized at 250 °C than in the washed 10.8% $Ru/\gamma\text{-}Al_2O_3$ catalyst after the same treatment, and amounts to about 71.5% and 65%, respectively. This may be due to the higher ruthenium dispersion in the former case as shown by chemisorption, TEM and XRD data. The higher Ru dispersion in samples of the 4.6% $Ru/\gamma\text{-}Al_2O_3$ catalyst is evidenced also by the XPS-determined Re/Al atomic ratios. As can be seen in Table 3, the $(Re/Al)_{XPS}$ atomic ratios for this catalyst were closer to the bulk atomic ratio, calculated from the overall chemical composition of the catalysts; $(Ru/Al)_{bulk} = 0.048$ for the 4.6% $Ru/\gamma\text{-}Al_2O_3$ catalyst and 0.122 for the 10.8% $Ru/\gamma\text{-}Al_2O_3$ catalyst, respectively. The calculated $(Cl/Ru)_{XPS}$ ratios for all studied samples are also presented in Table 3. As it can be seen, considerable amount of chlorine was retained on the surface of the unwashed catalysts and washing with hot water strongly decreases, but not eliminate completely, the chlorine content in these catalysts.

3.6. Catalytic activity

The oxidation of *n*-and *iso*-butane was performed with the reduced Ru/Al_2O_3 catalysts and with the same catalysts after oxidation treatment at 250 °C. The catalytic activity of the directly reduced Ru/Al_2O_3 catalysts for butane combustion was found to be significantly dependent on the washing procedures. For example, Fig. 6 shows the butane conversion over the washed and unwashed 4.6% Ru/Al_2O_3 catalyst as a function of temperature. It is clearly seen that the washing procedure leads to a dramatic enhancement in the catalytic activity of this catalyst. The characteristic temperature at which 50% conversion is reached ($T_{50\%}$) is over 130 °C lower for the washed sample (168 and 172 °C for *iso*- and *n*-butane, respectively) than for the unwashed one (300 and 312 °C for *iso*- and *n*-butane, respectively), and at 200 °C the conversion of *iso*- and *n*-butane is 20 and 100 times greater, respectively. Moreover, complete butane oxidation to CO_2 was observed at 190 and 400 °C for the washed and unwashed 4.6% Ru catalyst, respectively. Similar changes in activity were found for the washed and unwashed 10.8% Ru/Al_2O_3 catalyst, as it is indicated in Table 4. Additionally, as shown in Fig. 6, *iso*-butane combustion over the

Table 2
Oxygen uptake at room temperature and at 250 °C by the $Ru/\gamma\text{-}Al_2O_3$ catalysts.

Catalyst	O_2 uptake at RT (μmol O_2/g cat.)	O_2 uptake at 250 °C (μmol O_2/g cat.)	Calculated O_2 uptake to total oxidation of Ru to RuO_2 oxide (μmol O_2/g cat.)
3.5% $Ru/\gamma\text{-}Al_2O_3$ (calcined/reduced)	25	104	346.3
4.6% $Ru/\gamma\text{-}Al_2O_3$ (washed/reduced)	112	228	455.1
10.8% $Ru/\gamma\text{-}Al_2O_3$ (washed/reduced)	124	360	1068.5

Table 3
XPS atomic ratios obtained for the Ru/γ-Al_2O_3 catalysts after O_2 uptake measurements at room temperature and at 250 °C.

Catalyst	Treatment	Ru^0/Ru^{n+}	Ru/Al	Cl/Ru
4.6% Ru/γ-Al_2O_3[a] (unwashed)	H_2, 500 °C + O_2 uptake at RT	3.2	0.044	1.90
4.6% Ru/γ-Al_2O_3[a] (washed)	H_2, 500 °C + O_2 uptake at RT	1.9	0.033	0.27
4.6% Ru/γ-Al_2O_3 (washed)	H_2, 500 °C + O_2 uptake at 250 °C	0.40	0.034	0.26
10.8% Ru/γ-Al_2O_3 (unwashed)	H_2, 500 °C + O_2 uptake at RT	3.5	0.056	1.93
10.8% Ru/γ-Al_2O_3 (washed)	H_2, 500 °C + O_2 uptake at RT	1.75	0.059	0.45
10.8% Ru/γ-Al_2O_3 (washed)	H_2, 500 °C + O_2 uptake at 250 °C	0.52	0.060	0.43

[a] Data from ref. [48].

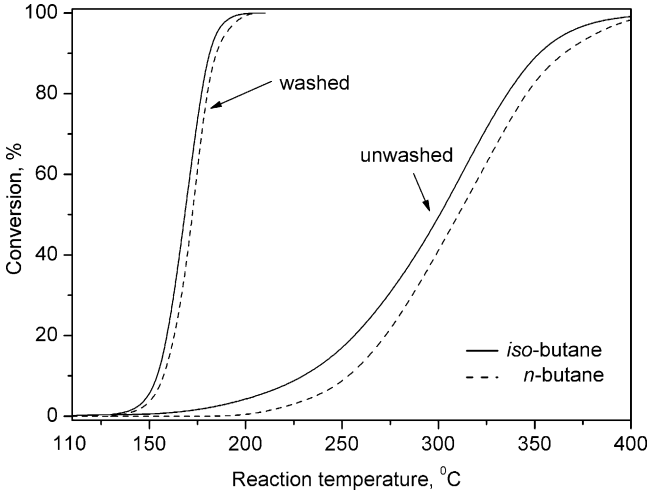

Fig. 6. Butane conversion over the reduced 4.6% Ru/γ-Al_2O_3 catalyst (washed and unwashed) as a function of reaction temperature.

both Ru/Al_2O_3 catalyst samples proceed at slightly lower temperature than *n*-butane combustion over the same catalysts. This higher activity can be explained by the weaker strength of the C–H bonds of the *iso*-butane and/or by a higher reactivity of oxygen species with *iso*-butane. Also, from the literature it is known that the rate-limiting activation in the alkane combustion is determined by the energy required to cleave the weakest C–H bond [50]. Johnson and Weinberg [51] found that the apparent C–H bond activation energy for the *iso*-butane is only a little lower than for *n*-butane (11.3 and 11.5 kcal/mol, respectively). For the washed catalyst sample conversion of butane increased rapidly as the reaction temperature increased what is also reflected in the Arrhenius plots shown in Fig. 7. Turnover frequencies values (TOF, molecules of *iso*-butane reacted per surface Ru per second) used in the Arrhenius plots were calculated from the activity data presented in Fig. 6 and hydrogen chemisorption results, by assuming that under conditions of excess oxygen butane combustion over Ru is first order in respect to C_4H_{10} and zero order in respect to O_2. From the Arrhenius plots, apparent activation energies of 34.9 and 14.3 kcal/mol for the Cl-free and Cl-containing catalyst, respectively, were obtained. Unexpectedly, more active catalyst exhibits higher apparent activation energy. Garetto et al. [52] also found for C_2–C_4 alkane oxidation that more active supported Pt/catalysts exhibit higher apparent activation energies and a compensation effect between the apparent activation energy and the preexpotencial factor has been verified. It can be noted that both Ru/Al_2O_3 catalysts have identical Ru loading, as well as, nearly the same average particle size (see Table 1), hence one of the possible factors affecting the catalyst activity could be the poisoning effect of the residual precursors remaining on the surface of the catalyst. The formation of the oxychloride species ($RuOCl_x$) on the surface of the ruthenium particles has been reported in the literature. As it was found by chemical analyses and XPS data (Tables 1 and 3), the large amount of chlorine was retained on the surface of the unwashed catalysts after H_2 reduction at 500 °C. Additionally, as it can be seen in Table 4, TOF at 175 °C for the both unwashed catalysts is much lower than that obtained for the chlorine-free 3.5% Ru/Al_2O_3 catalyst. Thus, the poisoning effect of chlorine on the Ru catalysts during combustion of butane is established. The poisoning effect of chlorine on the Pt and Pd-supported catalysts [53–55] during oxidation reactions is also well known.

The effect of Cl on butane combustion on Ru/Al_2O_3 catalysts exists, thus the further catalytic experiments were performed with the catalyst samples after removing chlorine ions. However, it can be noted that the washing of the Ru/Al_2O_3 catalysts with hot water markedly decreased the amount of Cl^- ions associated with the Ru surface but chlorine ions are still present on the γ-alumina support [36]. Fig. 8 shows the results obtained for the reduced Ru/Al_2O_3 catalysts with different ruthenium loadings. The activity results are also summarized in Table 4. Although both the 4.6% (Fig. 8,

Table 4
Temperatures (°C) required for 50% and 100% conversion of *iso*-butane and TOF at 175 °C on the reduced Ru/γ-Al_2O_3 catalysts.

Catalyst	Treatment	$T_{50\%}$	$T_{100\%}$	TOF[a] at 175 °C (s^{-1})
3.5% Ru/γ-Al_2O_3	Air, 400 °C + H_2, 500 °C	288	400	0.0007
4.6% Ru/γ-Al_2O_3 (washed)	H_2, 500 °C	168	190	0.0035
4.6% Ru/γ-Al_2O_3 (unwashed)	H_2, 500 °C	300	400	0.0002
10.8% Ru/γ-Al_2O_3 (washed)	H_2, 500 °C	170	220	0.0025
10.8% Ru/γ-Al_2O_3 (unwashed)	H_2, 500 °C	310	400	0.0001

[a] TOF, molecules of butane reacted per surface Ru per second at 175 °C.

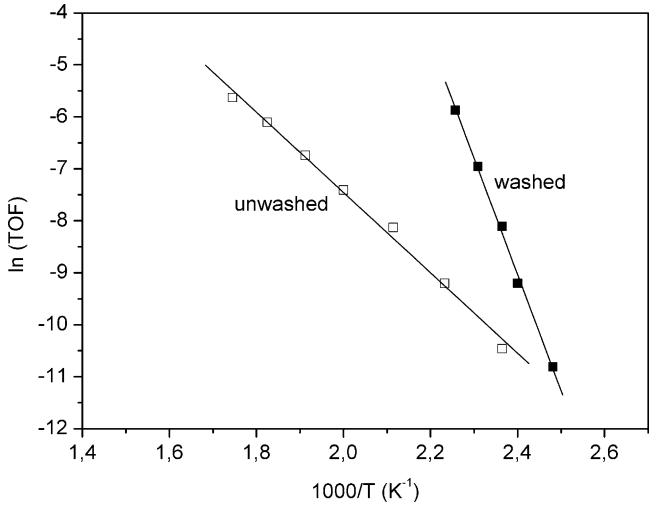

Fig. 7. Arrhenius plots for the *iso*-butane combustion over the 4.6% Ru/γ-Al_2O_3 washed (■) and unwashed catalyst (□).

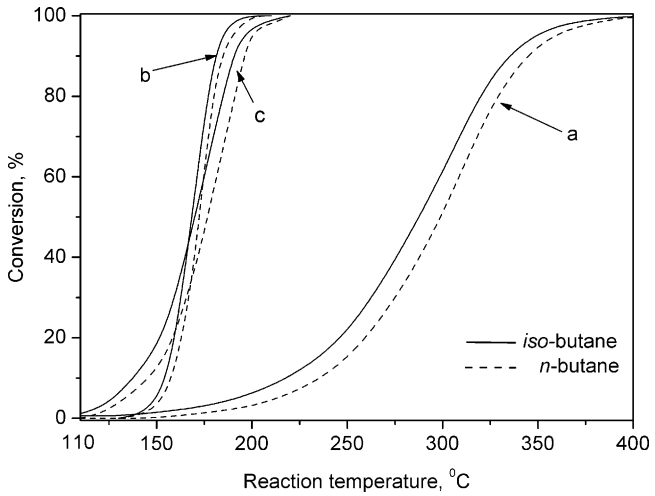

Fig. 8. Butane conversion over alumina supported ruthenium catalysts (after removing Cl ions) with different metal loadings as a function of reaction temperature (a) 3.5 wt.% Ru, (b) 4.6 wt.% Ru and (c) 10.8 wt.% Ru.

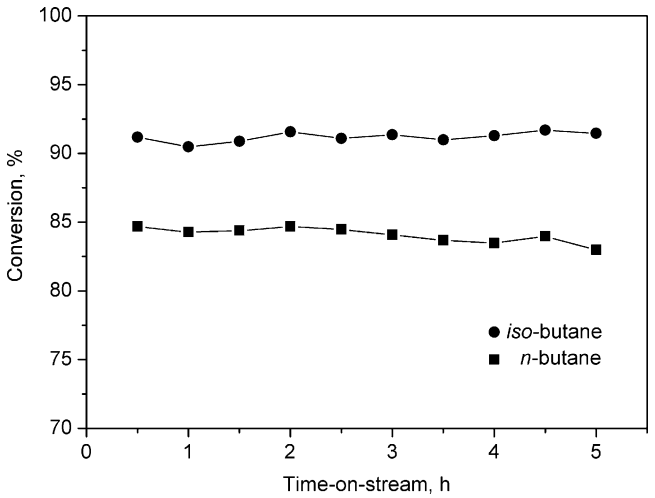

Fig. 9. Butane conversion over the reduced 10.8% Ru/γ-Al_2O_3 catalyst (washed) at 190 °C as a function of time on stream.

curve b) and 10.8% (Fig. 8, curve c) Ru catalysts give a light-off curves with the similar $T_{50\%}$ ~170 and 175 °C for *iso*- and *n*-butane, respectively, the first one showed initial steady state activity at higher temperature (above 130 °C) than the second one (below 110 °C) and conversion increased more rapidly as the reaction temperature increased. Complete butane conversion to CO_2 was observed at 190 and 210 °C for the 4.6% and 10.8% Ru catalyst, respectively. The small differences in the activity may indicate that the number of the active sites is similar in these samples. In fact, the specific active metal surface area calculated from the hydrogen chemisorption data, amounts to 5.2 and 6.0 m^2/g cat., for the 4.6% and 10.8% Ru/Al_2O_3 catalyst, respectively. The catalytic behavior of the 3.5% Ru catalyst (Fig. 8, curve a) was quite different and it was found to be considerably less active than others. These results can be attributed to the differences in the number of exposed active sites, which in turn depend on the pre-treatment of the catalysts, as evidenced by H_2 chemisorption, XRD and TEM data. Indeed, the 3.5% Ru/γ-Al_2O_3 was initially active at relatively low temperature (~150 °C), but butane conversion increased very slowly with temperature, giving 100% at 400 °C, while the corresponding $T_{50\%}$ were obtained at 288 and 300 °C for *iso*-butane and *n*-butane, respectively. Thus, this catalyst requires considerably higher temperature to obtain 50% conversion, i.e., above 120 °C as compared to the directly reduced samples. These activity results indicate that the pre-treatment procedures (calcination–reduction or direct reduction) have some influence, not only on dispersion or particle size of the metallic phase, but also on the catalytic performance of the Ru/γ-Al_2O_3 catalysts. Similar effect of the pre-treatment procedure on the CO oxidation over Ru/SiO_2 and Ru/Al_2O_3 was observed by Chin et al. [42]. Also, as shown in the last column of Table 4, the TOF calculated at 175 °C for the most active 4.6% catalyst (with dispersion H/Ru = 0.23), is five times higher as compared to the calcined–reduced 3.5% Ru catalyst (with dispersion H/Ru = 0.07). These data are in agreement with recent studies performed for the total oxidation of C_2–C_4 n-alkanes on supported Pt catalysts [52].

The evolution of the catalytic activity for butane oxidation reaction as a function of time on stream was also measured for the selected reduced catalyst samples, at constant temperature. For example, Fig. 9 shows butane conversion over the washed 10.8% Ru/Al_2O_3 catalyst as a function of time on stream at 190 °C. Catalyst stability test was carried out at temperature which resulted in conversion less than 100%, providing a more sensitive indication of changes of the catalyst performance with time on stream. It is observed that butane conversion does not change after 5 h time on line, thereby indicating high stability of the catalyst under oxygen-rich reaction conditions. Recently, no evidence for Ru oxidation was found in the 10.8% Ru/γ-Al_2O_3 catalyst oxidized at 100–200 °C, by using HRTEM, SAED and XRD methods [39]. Similar result was obtained for the 4.6% catalyst sample, thus no significant structural catalysts deactivation takes place on stream up to 200 °C.

To demonstrate the role of the degree of ruthenium oxidation on the butane combustion, the reduced Ru/γ-Al_2O_3 catalysts were next subjected to oxidation treatment at 250 °C. The activity of such treated samples was then monitored using the same conditions as were applied for the measurements with the initially reduced catalysts. Fig. 10 shows the effect of the oxidation treatment on the activity of the washed 4.6% Ru/γ-Al_2O_3 catalyst. As it can be seen, the activity of the catalyst oxidized at 250 °C was somewhat lower than that of the reduced one. Although both catalyst samples are initially active at the same temperature, oxidation of the reduced catalyst resulted in approximately 25 °C shift of the $T_{50\%}$ and the temperature of total combustion of butane. The similar changes in the catalytic activity were observed for the all studied Ru/γ-Al_2O_3 catalysts oxidized at 250 °C. The characterization data of the catalysts before activity studies show that at 250 °C, the small Ru particles in the Ru/Al_2O_3 catalysts were

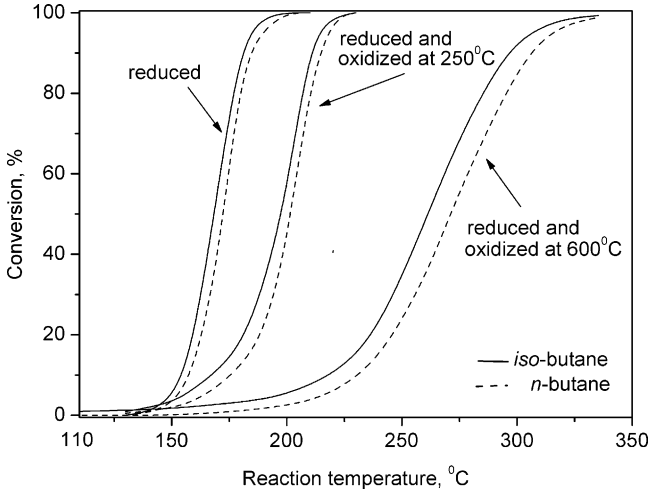

Fig. 10. Butane conversion over the 4.6% Ru/γ-Al_2O_3 catalyst (washed) after oxidation treatments at 250 and 600 °C as a function of reaction temperature.

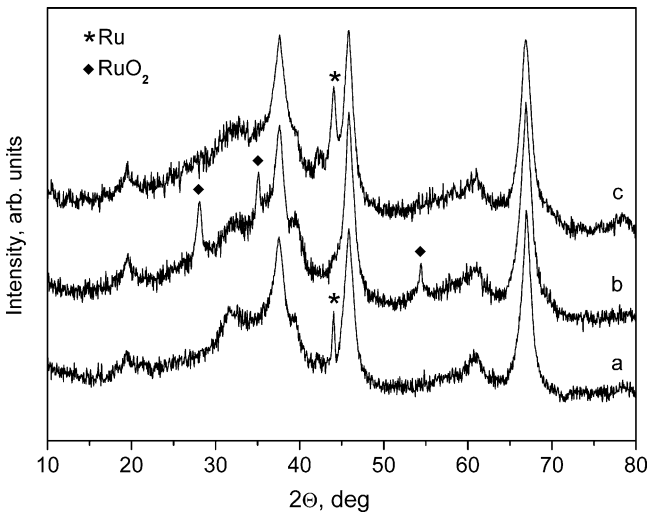

Fig. 11. X-ray diffraction patterns of the used catalysts with the metal loading of (a) 3.5 wt.% Ru, (b) 4.6 wt.% and (c) 10.8 wt.% Ru.

completely oxidized to small RuO_2 particles, whereas the large ruthenium particles were only covered with an ultra-thin poorly ordered layer of a ruthenium oxide. However, further increase in the oxidation temperature to 600 °C results in a sharp decrease in the catalytic activity, as shown in Fig. 10. These activity results are consistent with the recent studies of Mitsui et al. [32], who evidenced also that activity of the $Ru/\gamma\text{-}Al_2O_3$ and Ru/ZrO_2 catalysts for combustion of ethyl acetate, acetaldehyde and toluene was higher on the reduced catalysts than on the as-calcined at 400 °C. The much lower activity of the catalyst oxidized at 600 °C, may result not only from the sintering of the active phase, but also from the structural transformations of the catalyst. In fact, XRD data confirmed that in the sample oxidized at 600 °C, the Ru particles were completely oxidized to well-crystallized RuO_2 phase (not shown). The mean crystallite size of the RuO_2 oxide, calculated from corresponding X-ray diffraction pattern was estimated to be 9 nm and it was much higher than that of after oxidation at 250 °C (4–5 nm). Thus, some deactivation of supported Ru catalysts via the formation of well-crystallized RuO_2 oxide was found in our catalytic experiments. Deactivation of the supported Ru catalysts by the formation of RuO_2 was reported also by the early work of Kiss and Gonzalez [56] for CO oxidation under O_2-rich reaction conditions. However, more recent studies of the CO oxidation on the supported Ru catalysts and polycrystalline RuO_2/Ru powder showed that the deactivation mechanism is more complex [19].

3.7. Characterization of used catalysts

The used Ru catalysts, reduced in H_2 before activity measurements, were characterized by XRD and TEM methods. The post reaction characterization showed that the catalysts went through some structural changes during the combustion of butane in large excess of O_2. As shown in Fig. 11, the used 3.5% and 10.8% Ru catalysts exhibited the XRD patterns with the characteristic diffraction peak of metallic Ru phase ($2\Theta = 44.0^\circ$), similar as the fresh reduced catalysts (see Fig. 1, traces a and c). Thus, diffraction peaks due to the ruthenium oxide were not detected for these samples, indicating probably the high dispersion of the oxidized ruthenium species. However, for the used 4.6% catalyst, diffraction peaks of crystalline RuO_2 phase ($2\Theta = 28.0^\circ$, 35.1° and 54.3°) were clearly observed. Therefore, highly dispersed metallic ruthenium species present in the freshly reduced catalyst (X-ray amorphous as shown in Fig. 1, trace b), became oxidized by oxygen under the present reaction conditions. Additionally, some aggregation of the oxidized ruthenium species occurs under the reaction mixture, as it is evidenced by the increase in the intensity of the reflections of the RuO_2 phase in the used catalyst as compared to the fresh catalyst oxidized at 250 °C (compare Fig. 2b with Fig. 11b). Probably, some a hydrothermal sintering of the RuO_2 phase occurs under the reaction mixture.

Fig. 12 shows the TEM micrograph as well as a selected area electron diffraction pattern (as inset) and the corresponding particle size distribution of the used 10.8% $Ru/\gamma\text{-}Al_2O_3$ catalyst. As it can be seen the overall morphology of this catalyst is similar to that before activity test (Fig. 3c). The particles of ruthenium phase visible in the TEM image, as small and circular as well as larger, irregular dark particles, have similar sizes between 1.5 and 20 nm, though the mean particle size is slightly higher (4.8 nm) than in the fresh reduced catalyst (3.2 nm). Thus, some sintering of the ruthenium phase occurs under oxidation reaction conditions. The SAED pattern shows strong rings of the support, individual strong spots of the Ru metal and weak spots of the RuO_2 oxide. A HRTEM image of the used 10.8% $Ru/\gamma\text{-}Al_2O_3$ catalyst is presented in Fig. 13. As it can be seen, crystallites of metallic ruthenium covered with well-crystallized layer (with a thickness of about 2–3 nm) are accompanied by significantly smaller, poorly organized particles. These small particles are probably ruthenium oxide that was

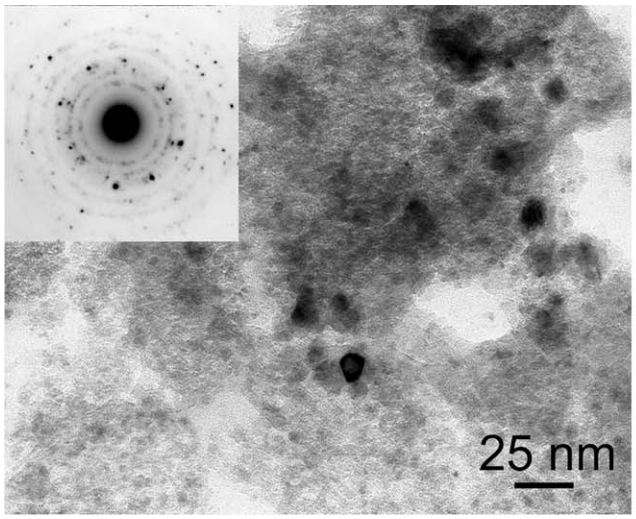

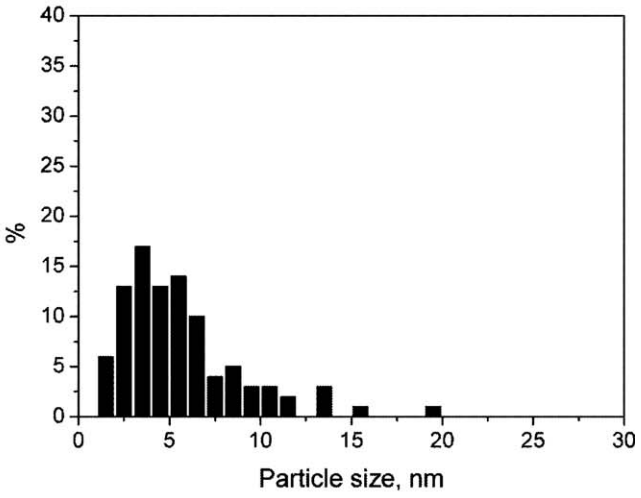

Fig. 12. TEM micrograph with SAED pattern (inset) and corresponding particle size distribution of the used 10.8% $Ru/\gamma\text{-}Al_2O_3$ catalyst.

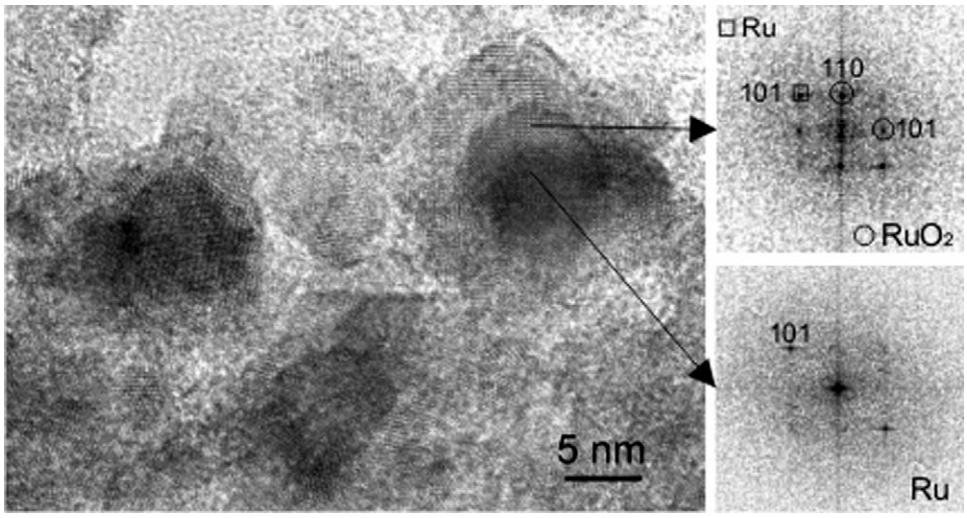

Fig. 13. HRTEM image of the ruthenium particles in the used 10.8% Ru/Al_2O_3 catalyst and FFT patterns from particle core and shell, respectively.

formed from the small Ru particles after exposing to reaction mixture. The fast Fourier transform (FFT) pattern from the core of the crystalline particles contains spots corresponding to 0.21 nm lattice fringes (Ru (1 0 1)), whereas FFT pattern from the overlayer contains spots corresponding to RuO_2 (1 0 1) and RuO_2 (1 1 0) as well as to Ru (1 0 1) (see insets in Fig. 13). These results are in agreement with the observation from XRD (Fig. 11c), which indicated the occurrence only Ru metal phase in this catalyst sample, since the ruthenium oxide phase was below detection limit of XRD method.

Summarizing the results of the catalytic activity and characterization data of the fresh and used catalysts we suppose that the most active sites in the butane oxidation reaction in large excess of air by the supported ruthenium catalysts, consist probably a few thick layer surface oxide on the large Ru particles and a small Ru_xO_y clusters without well-defined stoichiometry. Such surface species were formed at temperature of 100–200 °C in the most active reduced Cl-free 4.6% Ru catalyst, which reached 100% butane conversion below 200 °C (Fig. 6). From literature data it is known that the formation of a stoichiometric RuO_2 oxide is kinetically hindered at temperatures below 230 °C and occurs readily at higher temperatures [57]. In accord with these data, it was found recently for the 10.8% $Ru/\gamma\text{-}Al_2O_3$ catalyst by HRTEM and XRD, that at 100–200 °C the stoichiometric RuO_2 oxide was still not formed [39]. The present XRD and TEM studies showed that at 250 °C, poorly ordered RuO_2 with mean crystallite size of about 4–5 nm was formed, but large Ru particles were covered with very thin nearly amorphous oxide layer. Additionally, the catalytic results clearly show that the activity of the $Ru/\gamma\text{-}Al_2O_3$ catalysts for butane oxidation declined as the samples were oxidized at higher temperature, i.e., when the Ru oxidation degree increased (Fig. 10). As shown in Fig. 10, the 4.6% Ru catalyst in the fully oxidized state reached 100% butane conversion at about 350 °C. Therefore, our experimental data showed that under O_2-rich reaction conditions well below 250 °C the Ru_xO_y, while above 250 °C well-crystallized RuO_2 is the catalytically active phase. According to the literature data, the butane oxidation probably proceeds via the Mars-van Krevelen mechanism [18,23]. In the oxidation reaction, the compound being oxidized takes an oxygen atom from the surface and creates an oxygen vacancy. The rate determining step is the abstraction of the first hydrogen from butane leading to the adsorbed butane molecule and hydroxyl species. Water is formed by the recombination of surface hydroxyl groups followed by desorption. Butane adsorbed on the surface of the catalyst is then oxidized through reduction of the Ru_xO_y species creating an oxygen vacancy. These surface reaction sites are then reoxidized by the dissociative adsorption of gas-phase oxygen. Our catalytic results evidenced that the availability of oxygen from the poorly ordered Ru_xO_y species was much higher as compared to that from RuO_2 oxide what is probably caused by an increase in the Ru–O bond energy. In such a case, as it was found in the present study, higher temperature would be necessary for the oxidation of the chemisorbed C_4H_9–Ru–O_2 species.

4. Conclusions

In this study, the performances of the $Ru/\gamma\text{-}Al_2O_3$ catalysts on butane oxidation reaction were investigated. It was found that the pre-treatment procedures such as calcination–reduction or direct reduction in H_2 of the $Ru/\gamma\text{-}Al_2O_3$ catalysts have a significant influence on ruthenium dispersion and the catalytic activity. It was observed that presence of large amount of chlorine ions decreased metal dispersion value of the directly reduced catalysts. Similarly, activities of the catalysts towards the butane oxidation reaction were suppressed in the presence of chlorine. The directly reduced nearly Cl-free 4.6%$Ru/\gamma\text{-}Al_2O_3$ catalyst, with high Ru dispersion shows the best catalytic performance, among all catalysts investigated. Additionally, the reduced Ru catalysts with low Cl content exhibited higher activity than the same catalysts after oxidation treatments at 250 °C or at higher temperature. The changes in activities of the catalysts were attributed to the change in the Ru oxidation degree as the temperature oxidation increased, which may lead to an increase in the Ru–O bond energy. As a consequence, a decrease in the availability of oxygen from RuO_2 oxide to oxidize butane adsorbed species at given temperature occurs. Contrary, the large availability of oxygen from the Ru_xO_y species, which are formed under reaction conditions at lower temperature on the initially reduced Ru catalysts, resulted in an increase of the catalytic activity in butane oxidation reaction.

Acknowledgments

The authors thanks Mrs. L. Krajczyk for TEM study, Dr W. Tylus for XPS data and Mrs. A. Cielecka for help in adsorption measurements.

References

[1] P.S. Kulkarni, J.G. Crespo, C.A.M. Afonso, Environ. Int. 34 (2008) 139.
[2] A.C. Lewis, N. Carslaw, P.J. Marriott, R.M. Kinghorn, P. Morrison, A.L. Lee, K.D. Bartle, M.J. Pilling, Nature 405 (2000) 778.
[3] R. Atkinson, J. Arey, Chem. Rev. 103 (2003) 4605.

[4] A. Buekens, in: N. Bhaskar, G.St. Cholakov (Eds.), Pollution Control Technologies, Encyclopedia of Life Support Systems, Eolss Publishers, Oxford, UK, 2005.
[5] P. Papaefthimiou, T. Ioannides, X.E. Verykios, Appl. Catal. B: Environ. 15 (1998) 75.
[6] O. Demoulin, B. Le Clef, M. Navez, P. Ruiz, Appl. Catal. A: Gen. 344 (2008) 1.
[7] K. Okumura, T. Kobayashi, H. Tanaka, M. Niwa, Appl. Catal. B: Environ. 44 (2003) 325.
[8] F.J. Maldonado-Hodar, C. Moreno-Castilla, A.F. Perez-Cadenas, Appl. Catal. B: Environ. 54 (2004) 217.
[9] K. Everaert, J. Baeyens, J. Hazard. Mater. B 109 (2004) 113.
[10] Ch. Zhao, I.E. Wachs, J. Catal. 257 (2008) 181.
[11] P. Konova, M. Stoyanova, A. Naydenov, St. Christoskova, D. Mehandjiev, Appl. Catal. A: Gen. 298 (2006) 109.
[12] Y.-F. Han, L. Chen, K. Ramesh, E. Widjaja, S. Chilukoti, I.K. Surjami, J. Chen, J. Catal. 253 (2008) 261.
[13] D. Delimaris, T. Ioannides, Appl. Catal. B: Environ. (2008), doi: 10.1016/j.apcatb.2008.04.006.
[14] J.M. Zen, A.S. Kumar, J.Ch. Chen, J. Mol. Catal. A: Chem. 165 (2001) 177.
[15] N. López, J. Gómez-Segura, R.P. Marín, J. Pérez-Ramírez, J. Catal. 255 (2008) 29.
[16] I. Balint, A. Miyazaki, K. Aika, J. Catal. 220 (2003) 74.
[17] Y. Liu, F.-Y. Huang, J.-M. Li, W.-Z. Weng, Ch.-R. Luo, M.-L. Wang, W.-S. Xia, Ch.-J. Huang, H.-L. Wan, J. Catal. 256 (2008) 192.
[18] H. Over, Y.D. Kim, A.P. Seitsonen, S. Wendt, E. Lundgren, M. Schmid, P. Varga, A. Morgante, G. Ertl, Science 287 (2000) 1474.
[19] J. Assmann, V. Narkhede, N.A. Breuer, M. Muhler, A.P. Seitsonen, M. Knapp, D. Crihan, A. Farkas, G. Mellau, H. Over, J. Phys.: Condens. Matter 20 (2008) 184017.
[20] K. Reuter, M. Scheffler, Phys. Rev. B 73 (2006) 045433.
[21] Y. Wang, K. Jacobi, W.-D. Schoene, G. Ertl, J. Phys. Chem. B 109 (2005) 7883.
[22] M. Knapp, D. Crihan, A.P. Seitsonen, E. Lundgren, A. Resta, J.N. Andersen, H. Over, J. Phys. Chem. C 111 (2007) 5363.
[23] H. Liu, E. Iglesia, J. Phys. Chem. B 109 (2005) 2155.
[24] M. Dhakad, S. Rayalu, J. Subrt, S. Bakardjieva, T. Mitsuhashi, N. Labhsetwar, Curr. Sci. 92 (2007) 1125.
[25] A.C. Basagiannis, X.E. Verykios, Appl. Catal. B: Environ. 82 (2008) 77.
[26] T. Utaka, T. Okanishi, T. Takeguchi, R. Kikuchi, K. Eguchi, Appl. Catal. A: Gen. 245 (2003) 343.
[27] I. Balint, A. Miyazaki, K. Aika, J. Catal. 207 (2002) 66.
[28] A. Pintar, J. Batista, T. Tisler, Appl. Catal. B: Environ. 84 (2008) 30.
[29] N. Li, C. Descorme, M. Besson, Appl. Catal. B: Environ. 71 (2007) 262.
[30] S. Hosokawa, H. Kanai, K. Utani, Yo-ichi Taniquchi, Y. Saito, S. Imamura, Appl. Catal. B: Environ. 45 (2003) 181.
[31] J. Barbier Jr., L. Oliviero, B. Renard, D. Duprez, Catal. Today 75 (2002) 29.
[32] T. Mitsui, K. Tsutsui, T. Matsui, R. Kikuchi, K. Eguchi, Appl. Catal. B: Environ. 81 (2008) 56.
[33] S. Aouad, E. Saab, E. Abi-Aad, A. Aboukais, Kinet. Catal. 48 (2007) 835.
[34] S. Hosokawa, Y. Fujinami, H. Kanai, J. Mol. Catal. A: Chem. 240 (2005) 49.
[35] T.V. Choudhary, S. Banerjee, V.R. Choudhary, Appl. Catal. A: Gen. 234 (2002) 1.
[36] J. Okal, M. Zawadzki, L. Kępiński, L. Krajczyk, W. Tylus, Appl. Catal. A: Gen. 319 (2007) 202.
[37] J. Okal, Polish J. Chem. 81 (2007) 69.
[38] International Centre for Diffraction Date, ICDD, PDF-4+, 2005.
[39] J. Okal, Mater. Res. Bull. (2008), doi:10.1016/j.materresbull.2008.05.018.
[40] G.C. Bond, J.C. Slaa, J. Mol. Catal. A: Chem. 96 (1995) 163.
[41] Y.-F. Han, M. Kinne, R.J. Behm, Appl. Catal. B: Environ. 52 (2004) 123.
[42] S.Y. Chin, O.S. Alexeev, M.D. Amiridis, Appl. Catal. A: Gen. 286 (2005) 157.
[43] W. Vogel, N. Alonso-Vante, J. Catal. 232 (2005) 395.
[44] G.C. Bond, B. Coq, R. Dutartre, J.G. Ruiz, A.D. Hooper, M.G. Proietti, M.C.S. Sierra, J.C. Slaa, J. Catal. 161 (1996) 480.
[45] W. Rasband, ImageJ, U.S. National Institutes of Health, Bethesda, MD, USA, 1997–2005, http://rsb.info.nih.gov/ij/.
[46] K.C. Taylor, J. Catal. 38 (1975) 299.
[47] J.G. Goodwin Jr., J. Catal. 68 (1981) 227.
[48] J. Okal, Polish J. Chem. 81 (2007) 2181.
[49] J. Assmann, E. Löffler, A. Birkner, M. Muhler, Catal. Today 85 (2003) 235.
[50] A. O'Malley, B.K. Hodnett, Catal. Today 54 (1999) 31.
[51] D.F. Johnson, W.H. Weinberg, J. Chem. Phys. 103 (1995) 5833.
[52] T.F. Garetto, E. Rincón, C.R. Apesteguía, Appl. Catal. B: Environ. 73 (2007) 65.
[53] F.J. Gracia, J.T. Miller, A.J. Kropf, E.E. Wolf, J. Catal. 209 (2002) 341.
[54] U. Oran, D. Uner, Appl. Catal. B: Environ. 54 (2004) 183.
[55] D. Roth, P. Gelin, M. Primet, E. Tena, Appl. Catal. A: Gen. 203 (2000) 37.
[56] J.T. Kiss, R.D. Gonzalez, J. Phys. Chem. 88 (1984) 892.
[57] R. Blume, M. Hävecker, S. Zafeiratos, D. Teschner, E. Kleimenov, A. Knop-Gericke, R. Schlögl, A. Barinov, P. Dudin, M. Kiskinova, J. Catal. 239 (2006) 354.